1-1-2018

Yb^{3+} and Yb^{3+}/Er^{3+} doping for near-infrared emission and improved stability of CsPbCl3 nanocrystals

Xiangtong Zhang
Jilin University

Yu Zhang
Jilin University

Xiaoyu Zhang
Jilin University

Wenxu Yin
Jilin University

Yu Wang
Jilin University

See next page for additional authors

Recommended Citation

Zhang, X., Zhang, Y., Zhang, X., Yin, W., Wang, Y., Wang, H., Lu, M., Li, Z., Gu, Z., & Yu, W. (2018). Yb^{3+} and Yb^{3+}/Er^{3+} doping for near-infrared emission and improved stability of CsPbCl3 nanocrystals. *Journal of Materials Chemistry C*, 10101-10105. https://doi.org/10.1039/c8tc03957g

HHS Public Access

Author manuscript

J Mater Chem C Mater. Author manuscript; available in PMC 2018 November 29.

Published in final edited form as:

J Mater Chem C Mater. 2018 ; 6(37): 10101–10105. doi:10.1039/c8tc03957g.

Yb^{3+} and Yb^{3+}/Er^{3+} Doping for Near-Infrared Emission and Improved Stability of $CsPbCl_3$ Nanocrystals†

Xiangtong Zhang[a], **Yu Zhang**[a], **Xiaoyu Zhang**[b], **Wenxu Yin**[a], **Yu Wang**[a], **Hua Wang**[c], **Min Lu**[a], **Zhiyang Li**[d], **Zhiyong Gu**[d], and **William W. Yu**[c]

[a]State Key Laboratory of Integrated Optoelectronics and College of Electronic Science and Engineering, Jilin University, Changchun, 130012, China.

[b]School of Materials Science & Engineering, Jilin University, Changchun 130012, China

[c]Department of Chemistry and Physics, Louisiana State University, Shreveport, LA 71115, USA.

[d]Department of Chemical Engineering, University of Massachusetts Lowell, Lowell, MA 01854, USA

Abstract

Lead halide perovskite nanocrystals (NCs) exhibit excellent tunable emissions covering the entire visible spectral region, but they do not emit near-infrared (NIR) light. We synthesized rare earth element doped $CsPbCl_3$ NCs for NIR emission. The Yb^{3+} doped $CsPbCl_3$ NCs emitted strong 986 nm NIR light; the Yb^{3+}/Er^{3+} co-doped $CsPbCl_3$ NCs emitted at 1533 nm. The total photoluminescence quantum yield (PL QY) of the $CsPbCl_3$ NCs changed from 5.0% to 127.8% upon incorporating 2.0% Yb^{3+}, a factor of 25.6 times enhancement. The material's stability was tested under continuous ultraviolet (365 nm) irradiation. The doped $CsPbCl_3$ NCs exhibited a better stability than the undoped one. The PL intensity of the undoped $CsPbCl_3$ NCs dropped to 20% of the initial value in 27 h, while the doped one took 85 h.

Introduction

With facile tunability of emission over the whole visible spectrum, nonblinking characteristic, large absorption coefficient, narrow emission line widths and near-unit quantum yields (QYs),[1–6] lead halide perovskite nanocrystals (NCs) have attracted intensive attention as excellent materials for a wide range of applications including high-efficient solar cells,[7] light-emitting diodes and lasing.[8–13] Perovskite NCs with a formula $APbX_3$ [A = Cs^+, $CH_3NH_3^+$, or $CH(NH_2)_2^+$; X = Cl^-, Br^-, I^-, or their mixtures]obey the tolerance factor and octahedral factor in structures.[14–16] These two factors also make these perovskite NCs tolerant to doped elements. Doping is an effective way to adjust the electronic and optical performances or to improve the stability.[17,18] In fact, many reports have validated the facile doping in lead halide perovskites due to their non-rigid structures. For example, Ag^+, K^+, Rb

†Electronic supplementary information (ESI) available: XPS spectra, XRD patterns and optical spectra. See DOI: 10.1039/c8tc03957g

Corresponding authors: yuzhang@jlu.edu.cn (Y. Zhang), wyu6000@gmail.com (W. W. Yu).

Conflicts of interest

There are no conflicts to declare.

$^{+}$, Sn^{4+}, Sn^{2+}, Zn^{2+}, Cd^{2+}, Bi^{3+} and Mn^{2+} have been applied as dopants,[19–26] but none of them can enable near-infrared (NIR) emissions.

Rare earth (RE) elements usually act as PL centers in many host materials such as oxides, fluorides and semiconductors.[27–30] Owing to the strong shielding effect from the eight electrons in their outer 5s and 5p electronic orbitals, the partially filled 4f electronic orbital have various energy levels. These electrons jumping among the different energy levels generate various narrow width emissions ranging from UV to IR and thus there are many useful applications such as multimodal imaging probes, temperature sensing, lighting devices and theranostics.[31–35] The luminescence of RE ions can be sensitized by various energy transfer channels.[36] There are mainly two reasons for $CsPbCl_3$ NCs to be chosen as a luminescent acceptor: lead halide perovskites have large absorption coefficients;[6] $CsPbCl_3$ NCs have a large band gap among lead halide perovskites, which is appropriate for exciton energy transfer.[37] It is highly desirable to successfully link the absorption of lead halide perovskite NCs and the IR emission of RE elements.

Recently, Pan *et al.* doped several lanthanide elements into $CsPbCl_3$ NCs and showed interesting changes.[38] Milstein *et al.* provided insights into the microscopic mechanism behind the extremely efficient sensitization of Yb^{3+} luminescence in $CsPbX_3$ NCs.[39] Here, we report a successful synthesis of colloidal $CsPbCl_3$:Yb^{3+}, $CsPbCl_3$:Er^{3+} and $CsPbCl_3$:Yb^{3+}/Er^{3+} NCs by a modified hot-injection method, which is simpler and more effective. The optimal doping level was 2.0% for the $CsPbCl_3$:Yb^{3+} NCs; the total photoluminescence (PL) QY was 127.8% with both the band edge and 986 nm NIR emissions. Besides, we also acquired emission at 1533 nm from the Yb^{3+}/Er^{3+} co-doped $CsPbCl_3$ NCs. These doped NCs may be applied to NIR diode lasers and photo-communications.

Experimental

Materials

Cs_2CO_3 (99.995%, Sigma-Aldrich), 1-octadecene (ODE, technical grade 90%, Sigma-Aldrich), oleic acid (OA, technical grade 90%, Sigma-Aldrich), oleylamine (OAm, 80–90%, Aladdin), lead acetate trihydrate ($Pb(OAc)_23H_2O$, 99.99% metal basis, Aladdin), lead(II) chloride ($PbCl_2$, 99.999% metal basis, Sigma-Aldrich), ytterbium chloride hexahydrate ($YbCl_36H_2O$, 99.9% metal basis, Aladdin), erbium chloride hexahydrate ($ErCl_36H_2O$, 99.9% metal basis, Aladdin), and toluene (GR, Beijing Chemical Reagent Ltd) were used as received.

Preparation of Cs-oleate solution

A cesium-oleate solution was prepared according to the approach reported by Protesescu *et al.*[1] Briefly, 0.814 g of Cs_2CO_3, 2.5 ml of OA and 30 ml of ODE were loaded in a 100 ml three-neck round bottom flask and degassed under vacuum at 120 °C for 1 h. Then, the flask was filled with flowing N_2 gas and heated up to 150 °C until all Cs_2CO_3 reacted with OA. The solution was then cooled down to room temperature naturally and stored under N_2 protection.

Preparation of the $CsPbCl_3$ NCs

$PbCl_2$ (0.376 mmol), OA (1 ml), OAm (1 ml) and ODE (10 ml) were added to a 50 ml three-neck round bottom flask and dried under vacuum at 120 °C for 1 h. Then the temperature was increased to 180 °C under flowing N_2. A preheated (100 °C) 0.8 ml Cs-oleate solution was swiftly injected using a syringe. After 5 s, the flask was immersed in an ice bath to stop the reaction.

Preparation of the single doped $CsPbCl_3$ NCs with Yb^{3+} or Er^{3+}

Typically, 0.376 mmol of $YbCl_3{\cdot}6H_2O$ (or $ErCl_3{\cdot}6H_2O$) and 0.123 mmol of $Pb(OAc)_2{\cdot}3H_2O$ were mixed with 2 ml of OA, 2 ml of OAm and 10 ml of ODE in a 50 ml quartz three-neck round bottom flask. After being degassed under vacuum at 120 °C for 1 h, the reactants were completely dissolved and the flask was switched to a N_2 atmosphere. The temperature was quickly increased to 260 °C and maintained for 3 min. Then, a preheated (100 °C) 0.8 ml Cs-oleate solution was swiftly injected *via* a syringe. 5 s later, the flask was immersed into an ice bath to stop the reaction. It should be pointed out that a quartz flask was used to tolerate the quick temperature change from 260 °C to 0 °C.

Preparation of the co-doped $CsPbCl_3$ NCs with Yb^{3+} and Er^{3+}

All steps and quantities were the same as those for the single doped $CsPbCl_3$ NCs except there was a mixture of two RE precursors with various molar ratios between $YbCl_3{\cdot}6H_2O$ and $ErCl_3{\cdot}6H_2O$. The ratios of Yb : Er were 8 : 2, 7 : 3, 6 : 4, and 5 : 5, respectively.

Purification

Firstly, the crude solution was centrifuged at 5000 rpm for 10 min to discard the supernatant. Secondly, the precipitate was dispersed in 5 ml of toluene and then centrifuged at 12000 rpm for 10 min. Lastly, the collected precipitate was dispersed in 3 ml of toluene and centrifuged at 3000 rpm for 2 min to remove all large particles; the final pure NCs were in the supernatant.

Characterization

Fluorescence emission spectra were measured using an Omni-λ 300 monochromator/spectrometer from Zolix. Absorbance spectra were recorded by using a Shimadzu UV-2550 spectrophotometer. The morphologies of the NCs were observed using a Tecnai F20 transmission electron microscope (TEM). The actual doping levels and ratios were found using a Varian 720-ES inductively coupled plasma-optical emission spectrometer (ICP-OES). X-ray diffraction (XRD) patterns of the NCs were acquired using a Bruker D8 Advance X-ray diffractometer (Cu Kα, λ = 1.5406 Å). X-ray photoelectron spectroscopy (XPS) was performed using an ESCALAB 250 spectrometer. The visible absolute PL QYs of the samples were determined using an FLS920P fluorescence spectrometer (Edinburgh Instruments) equipped with an integrating sphere with its inner face coated with BENFLEC. Time-resolved PL lifetime measurements were carried out using a time-correlated single-photon counting (TCSPC) lifetime spectroscopy system with a picosecond pulsed diode laser (EPL-365 nm) as the single wavelength excitation light source. A comparison of the luminescence intensity of the Yb^{3+} ions and the band edge emission of the $CsPbCl_3$ NCs

was done using an Ocean Optics spectrometer (QE-Pro) for the measurement of the NIR PL QYs.

Results and discussion

All samples were characterized by UV-visible absorption and PL (excited using 365 nm UV light) spectroscopies. The as-prepared $CsPbCl_3$ NCs showed band edge absorption and luminescence spectra similar to a previous report (Fig. 1a).[40] For the doped $CsPbCl_3$ NCs, there are some little blue shifts. According to the Burstein–Moss effect in heavily doped n-type semiconductors, slight blue shifts of both absorption and PL positions can be attributed to the filling of the state by the donated electrons of Yb^{3+} around the bottom of the conduction band, which leads to some band gap widening.[41] Their powder XRD patterns confirmed that their crystal structure still adopts the tetragonal phase (JCPDS No. PDF#18–0366) with the space group *P4mm* (Fig. 1b). There were some minor diffraction peaks (marked with *) that could be attributed to $Cs_3Pb_{6.48}Cl_{16}$ (JCPDS No. PDF#45–1243) or Cs_4PbCl_6 (JCPDS No. PDF#73–2477) formed at a reaction temperature of 220 °C and disappeared at higher temperatures. Besides, the peaks of other compounds, such as CsCl, $YbCl_3$, and $PbCl_2$, were not detected. The peak position of the (101) lattice plane shifted a little compared with that of the undoped sample (see the amplified view). For the samples synthesized at 260 °C and 280 °C, the peak positions progressively shifted to higher degrees, which is due to the shrinkage of the crystal lattice because of the incorporation of Yb^{3+} with a smaller ionic radius (0.086 nm) than Pb^{2+} (0.119 nm). Fig. 1c shows that the emission of the $^2F_{5/2}$–$^2F_{7/2}$ transition of the Yb^{3+} ions located at 986 nm with a full width at half maximum (FWHM) of 54 nm synthesized at different reaction temperatures. By using a high-resolution Omni-λ 500 spectrometer, a clear Stark split could be observed, as shown in Fig. S1 (ESI†). Obviously, when the reaction temperature was higher than 260°C, the intensity of the Yb^{3+} emission began to decrease (Fig. 1d). We attribute this phenomenon to the effect of concentration quenching just like the other lanthanide doped materials.[42]

We synthesized uniform cube-shaped $CsPbCl_3$ and $CsPbCl_3$:Yb^{3+} NCs with similar size distributions of around 10 nm (Fig. 2a, b, d and e). The HRTEM observations also confirmed the lattice contraction, which was initially found from XRD. The wellresolved lattice fringes of the highly crystalline structures of the $CsPbCl_3$ and $CsPbCl_3$:Yb^{3+} NCs are ascertained to be 3.96 and 3.92 Å, respectively (Fig. 2c and f). Combined with the results of XRD and HRTEM, the Yb^{3+} ions were successfully doped into the crystal structure of the $CsPbCl_3$ NCs.

Because of the low atomic content of Yb^{3+} ions (2.0% as determined by ICP-OES), the XPS tests failed to detect the signal of the Yb^{3+} ions on the surface (Fig. S2a, ESI†). Similar results were also reported by Nam *et al.,* wherein they did not find K^+ on the surface of their $Cs_{0.925}K_{0.075}PbI_2Br$ crystals.[19] Due to the lattice contraction in the $CsPbCl_3$:Yb^{3+} NCs, the chemical bonding properties among the crystal structures should have obvious changes.[43] Fig. 2 g-i show that the binding energies of the Cs^+, Pb^{2+} and Cl^- ions become higher. For Cs 3d, it changed from 724.1 to 724.3 eV; for Pb 4f, it shifted from 138.2 to 138.3 eV; for Cl

†Electronic supplementary information (ESI) available: XPS spectra, XRD patterns and optical spectra. See DOI: 10.1039/c8tc03957g

2p, a change from 197.6 to 197.9 eV was found. The whole XPS spectra of the $CsPbCl_3$ and $CsPbCl_3$:Yb^{3+} NCs are shown in Fig. S2b (ESI†). These shifts should be attributed to the doping of Yb^{3+} ions into the $CsPbCl_3$ NCs. The smaller Yb^{3+} ions could occupy the Pb-sites and form smaller octahedrons, leading to stronger chemical bonds among the Cs^+, Pb^{2+} and Cl^- ions. These changes also improve the stability of the Yb^{3+} ion doped $CsPbCl_3$ NCs (discussed later).

Luminescence decay–time measurements provide additional evidence for successful insertion of Yb^{3+} ions inside the internal lattices of the $CsPbCl_3$ NCs. Since the surface of the $CsPbCl_3$ NCs has many OA and OAm ligands, they readily diminish the NIR luminescence of Yb^{3+} by the vibrations of the C–H, N–H, or O–H bonds.[44] They can also lead to shortened excited-state decay times and lower the PL QYs, if the Yb^{3+} ions are closely adjacent to the ligands.[45] From the time-resolved PL decay tests, the luminescence decay–time of the $^2F_{5/2}$–$^2F_{7/2}$ transition of the Yb^{3+} ions inside the $CsPbCl_3$ NCs was found to be 941.9 μs (Fig. 3a). This value was similar to 815.0 μs of the Yb^{3+}-doped $PbIn_2S_4$ NCs and much longer than that of typical Yb^{3+} organic ligands complexes (~10 μs).[44,45] Besides, Fig. 3b shows that the incorporation of Yb^{3+} into $CsPbCl_3$ increases the average life time of the band edge emission of the $CsPbCl_3$ NCs from 3.9 to 8.2 ns. For the undoped $CsPbCl_3$ NCs, the fitted results reveal a τ_1 of 0.7 ns (accounting for 78.8%) and a τ_2 of 11.2 ns (accounting for 21.2%). For the $CsPbCl_3$:Yb^{3+} NCs, the fitted results reveal a τ_1 of 1.2 ns (accounting for 53.6%) and a τ_2 of 16.3 ns (accounting for 46.4%). This slightly increased average life time elevated the band edge emission PL QY from 5.0% to 7.7%, which may be attributed to some Cl vacancies passivated by doping with the metal ions.[38] The highest PL QY of NIR emission from Yb^{3+} was 120.1%, calculated by a comparison of the intensity with the intrinsic excitonic emission of the $CsPbCl_3$:Yb^{3+} NCs. The integral intensity contrast spectrum acquired using a fiber optic spectrometer is shown in Fig. S3 (ESI†).

Through individually monitoring the two emission peaks from the $CsPbCl_3$:Yb^{3+} NCs synthesized at 260 °C, we acquired two consistent excitation spectra (Fig. 4a and b). The difference of testing ranges between them is to avoid the detection of elastic scattering of the excitation source. Therefore, the wavelength testing ranges should have no overlap with the band edge emission of the $CsPbCl_3$:Yb^{3+} NCs. Since Yb^{3+} ions do not exhibit characteristic absorption in the UV through visible range, the excitation spectrum monitored at NIR emission of Yb^{3+} ions should be derived from the $CsPbCl_3 \rightarrow Yb^{3+}$ energy transfer. The huge PL QY difference between the visible and NIR emissions may be attributed to the quantum cutting, and we drew an energy level chart (Fig. 4c) to explain this process.[38] Similar to the structured isoelectronic traps of a lanthanide ion doped GaN semiconductor,[46] the incorporation of Yb^{3+} ions may generate a defect state in the middle of the band gap of the $CsPbCl_3$ NCs. When the $CsPbCl_3$:Yb^{3+} NCs were excited using 365 nm light, the $CsPbCl_3$ host generated excitons and they recombined through band gaps and emitted 408 nm light. Besides, the defect state induced by the Yb^{3+} ions divided the excitonic energy into two parts. One part of the energy transferred to the first Yb^{3+} ion. Then electrons were captured by the defect state through the Auger non-radiative relaxation process. The remaining energy was released by the exciton recombined between the electron on the defect state and the hole of the valence band. This energy further excited the second Yb^{3+} ion

through an Auger non-radiative energy transfer. For the excited Yb^{3+} ions, the electrons of the $^2F_{5/2}$ level jumped to the $^2F_{7/2}$ level and generated 986 nm photons.

The photostability of the NC solutions was tested at the same concentration under continuous irradiation with a 6 W UV (365 nm) lamp. The results are shown in Fig. 5. In about 27 h, the PL intensity of the undoped $CsPbCl_3$ NC solution decreased by 80%, whereas it took 85 h for the $CsPbCl_3$:Yb^{3+} NC solution to lose 80% of its PL intensity. The stability shows a great improvement because of Yb^{3+} doping.

We extended the method to synthesize Er^{3+} and Yb^{3+}/Er^{3+} doped $CsPbCl_3$ NCs. The XRD and optical characterization results of the $CsPbCl_3$:Er^{3+} and $CsPbCl_3$:Yb^{3+}/Er^{3+} NCs are shown in Fig. S4-S7 (ESI†), respectively. Interestingly, for the single doped $CsPbCl_3$:Er^{3+} NCs, we detected a wide-peak at 591 nm with an FWHM of 77 nm but failed to observe luminescence in the NIR range, which may be due to the formation of defect states in the band gap of the $CsPbCl_3$ NCs caused by Er^{3+}. However, for the double doped $CsPbCl_3$:Yb^{3+}/Er^{3+} NCs, a luminescence peak at 1533 nm (an FWHM of 34 nm) was obtained from the $^4I_{13/2}$–$^4I_{15/2}$ transition of the Er^{3+} ions. This phenomenon may be attributed to doping with the Yb^{3+} ions, which suppresses the emission from the defect states and builds an energy bridge between the $CsPbCl_3$ host and the Er^{3+} ions. Therefore, the excitation spectrum of the $CsPbCl_3$:Er^{3+}/Yb^{3+} NCs monitored at 1533 nm is similar to Fig. 4a and b (Fig. S6, ESI†). Fig. S5b (ESI†) shows the PL intensity changes at different feed ratios of Yb^{3+} to Er^{3+} ions under the same synthesis conditions. At a feed ratio of 7:3, we acquired the strongest NIR emission.

Conclusions

In conclusion, we have designed a feasible synthesis process to get high-efficient NIR emission with a PL QY of 127.8% ($CsPbCl_3$:Yb^{3+} NCs) with improved stability. The difference between the undoped and doped $CsPbCl_3$ NCs was discussed. The 986 nm NIR emission of Yb^{3+} and 1533 nm NIR emission of Er^{3+} may have potential for applications in diode lasers and photo-communications.

Supplementary Material

Refer to Web version on PubMed Central for supplementary material.

Acknowledgements

We acknowledge the following financial support from the National Key Research and Development Program of China (2017YFB0403601), the National Natural Science Foundation of China (61675086, 61475062, 61722504, 51772123, 51702115), the State Scholarship Fund of China Scholarship Council, the China Postdoctoral Science Foundation (2017M611319), the National Postdoctoral Program for Innovative Talents (BX201600060), the BORSF Professorship, Institutional Development Award (P20GM103424), the Special Project of the Province-University Co-constructing Program of Jilin Province (SXGJXX2017–3) and the Open Research Fund of State Key Laboratory of Polymer Physics and Chemistry, Changchun Institute of Applied Chemistry, Chinese Academy of Sciences.

References

1. Protesescu L, Yakunin S, Bodnarchuk MI, Krieg F, Caputo R, Hendon CH, Yang RX, Walsh A and Kovalenko MV, Nano Lett, 2015, 15, 3692–3696. [PubMed: 25633588]
2. Hu F, Yin C, Zhang H, Sun C, Yu WW, Zhang C, Wang X, Zhang Y and Xiao M, Nano Lett, 2016, 16, 6425–6430.
3. Liu F, Zhang Y, Ding C, Kobayashi S, Izuishi T, Nakazawa N, Toyoda T, Ohta T, Hayase S, Minemoto T, Yoshino K, Dai S and Shen Q, ACS Nano, 2017, 11, 10373–10383. [PubMed: 28910074]
4. Di Stasio F, Christodoulou S, Huo N and Konstantatos G, Chem. Mater, 2017, 29, 7663–7667.
5. Smith MD and Karunadasa HI, Acc. Chem. Res, 2018, 51, 619–627. [PubMed: 29461806]
6. Green MA, Ho-Baillie A and Snaith HJ, Nat. Photonics, 2014, 8, 506.
7. Liang J, Wang C, Wang Y, Xu Z, Lu Z, Ma Y, Zhu H, Hu Y, Xiao C, Yi X, Zhu G, Lv H, Ma L, Chen T, Tie Z, Jin Z and Liu J, J. Am. Chem. Soc, 2016, 138, 15829–15832. [PubMed: 27960305]
8. Cai P, Wang X, Seo HJ and Yan X, Appl. Phys. Lett, 2018, 112, 153901.
9. Wu H, Zhang Y, Lu M, Zhang X, Sun C, Zhang T, Colvin VL and Yu WW, Nanoscale, 2018, 10, 4173–4178. [PubMed: 29436554]
10. Wang P, Bai X, Sun C, Zhang X, Zhang T and Zhang Y, Appl. Phys. Lett, 2016, 109, 063106.
11. Wu H, Zhang Y, Zhang X, Lu M, Sun C, Zhang T and Yu WW, Adv. Opt. Mater, 2017, 5, 1700377.
12. Wang Y, Li X, Song J, Xiao L, Zeng H and Sun H, Adv. Mater, 2015, 27, 7101–7108. [PubMed: 26448638]
13. Chin XY, Perumal A, Bruno A, Yantara N, Veldhuis SA, Martínez-Sarti L, Chandran B, Chirvony V, Lo AS-Z, So J, Soci C, Gra¨tzel M, Bolink HJ, Mathews N and Mhaisalkar SG, Energy Environ. Sci, 2018, 11, 1770–1778.
14. Goldschmidt VM, Naturwissenschaften, 1926, 14, 477–485.
15. Li C, Lu X, Ding W, Feng L, Gao Y and Guo Z, Acta Crystallogr., Sect. B: Struct. Sci, 2008, 64, 702–707.
16. Travis W, Glover ENK, Bronstein H, Scanlon DO and Palgrave RG, Chem. Sci, 2016, 7, 4548–4556. [PubMed: 30155101]
17. Akkerman QA, Meggiolaro D, Dang Z, De Angelis F and Manna L, ACS Energy Lett, 2017, 2, 2183–2186. [PubMed: 29142911]
18. Zou S, Liu Y, Li J, Liu C, Feng R, Jiang F, Li Y, Song J, Zeng H, Hong M and Chen X, J. Am. Chem. Soc, 2017, 139, 11443–11450. [PubMed: 28756676]
19. Nam JK, Chai SU, Cha W, Choi YJ, Kim W, Jung MS, Kwon J, Kim D and Park JH, Nano Lett, 2017, 17, 2028–2033. [PubMed: 28170276]
20. Saliba M, Matsui T, Domanski K, Seo J-Y, Ummadisingu A, Zakeeruddin SM, Correa-Baena J-P, Tress WR, Abate A, Hagfeldt A and Grätzel M, Science, 2016, 354, 206. [PubMed: 27708053]
21. Wang HC, Wang W, Tang AC, Tsai HY, Bao Z, Ihara T, Yarita N, Tahara H, Kanemitsu Y, Chen S and Liu RS, Angew. Chem., Int. Ed, 2017, 56, 13650–13654.
22. Van der Stam W, Geuchies JJ, Altantzis T, van den Bos KH, Meeldijk JD, Van Aert S, Bals S, Vanmaekelbergh D and de Mello Donega C, J. Am. Chem. Soc, 2017, 139, 4087–4097. [PubMed: 28260380]
23. Liu H, Wu Z, Shao J, Yao D, Gao H, Liu Y, Yu W, Zhang H and Yang B, ACS Nano, 2017, 11, 2239–2247. [PubMed: 28145697]
24. Guria AK, Dutta SK, Adhikari SD and Pradhan N, ACS Energy Lett, 2017, 2, 1014–1021.
25. Shao H, Bai X, Cui H, Pan G, Jing P, Qu S, Zhu J, Zhai Y, Dong B and Song H, Nanoscale, 2018, 10, 1023–1029. [PubMed: 29265121]
26. Lu M, Zhang X, Bai X, Wu H, Shen X, Zhang Y, Zhang W, Zheng W, Song H, Yu WW and Rogach AL, ACS Energy Lett, 2018, 3, 1571–1577.
27. Zhang X, Fu Z, Sun Z, Liu G, Jeong JH and Wu Z, Opt. Mater, 2016, 60, 526–532.
28. Wang F and Liu X, Chem. Soc. Rev, 2009, 38, 976–989. [PubMed: 19421576]

29. Martín-Rodríguez R, Geitenbeek R and Meijerink A, J. Am. Chem. Soc, 2013, 135, 13668–13671. [PubMed: 24000937]
30. Chen D, Wan Z, Zhou Y, Zhou X, Yu Y, Zhong J, Ding M and Ji Z, ACS Appl. Mater. Interfaces, 2015, 7, 19484–19493. [PubMed: 26287513]
31. Bunzli J-CG and Piguet C, Chem. Soc. Rev, 2005, 34, 1048–1077. [PubMed: 16284671]
32. Jia M, Liu G, Sun Z, Fu Z and Xu W, Inorg. Chem, 2018, 57, 1213–1219. [PubMed: 29336559]
33. Wilhelm S, ACS Nano, 2017, 11, 10644–10653. [PubMed: 29068198]
34. Wang X, Liu Q, Cai P, Wang J, Qin L, Vu T and Seo HJ, Opt. Express, 2016, 24, 17792–17804. [PubMed: 27505747]
35. Wang X, Wang Y, Bu Y, Yan X, Wang J, Cai P, Vu T and Seo HJ, Sci. Rep, 2017, 7, 43383. [PubMed: 28240270]
36. Dong H, Sun L-D and Yan C-H, Chem. Soc. Rev, 2015, 44, 1608–1634. [PubMed: 25242465]
37. Guria AK, Dutta SK, Adhikari SD and Pradhan N, ACS Energy Lett, 2017, 2, 1014–1021.
38. Pan G, Bai X, Yang D, Chen X, Jing P, Qu S, Zhang L, Zhou D, Zhu J, Xu W, Dong B and Song H, Nano Lett, 2017, 17, 8005–8011. [PubMed: 29182877]
39. Milstein TJ, Kroupa DM and Gamelin DR, Nano Lett, 2018, 18, 3792–3799. [PubMed: 29746137]
40. Wu H, Zhang Y, Zhang X, Lu M, Sun C, Bai X, Zhang T, Sun G and Yu WW, Adv. Electron. Mater, 2018, 4, 1700285.
41. Yao J-S, Ge J, Han B-N, Wang K-H, Yao H-B, Yu H-L, Li J-H, Zhu B-S, Song J-Z, Chen C, Zhang Q, Zeng H-B, Luo Y and Yu S-H, J. Am. Chem. Soc, 2018, 140, 3626–3634. [PubMed: 29341604]
42. Zhang J, Hao Z, Li J, Zhang X, Luo Y and Pan G, Light: Sci. Appl, 2015, 4, e239.
43. Zhou D, Liu D, Pan G, Chen X, Li D, Xu W, Bai X and Song H, Adv. Mater, 2017, 29, 1704149.
44. Creutz SE, Fainblat R, Kim Y, De Siena MC and Gamelin DR, J. Am. Chem. Soc, 2017, 139, 11814–11824. [PubMed: 28750510]
45. Hou Y, Shi J, Chu W and Sun Z, Eur. J. Inorg. Chem, 2013, 3063–3069.
46. Dorenbos P and Kolk E. v. d., Appl. Phys. Lett, 2006, 89, 061122.

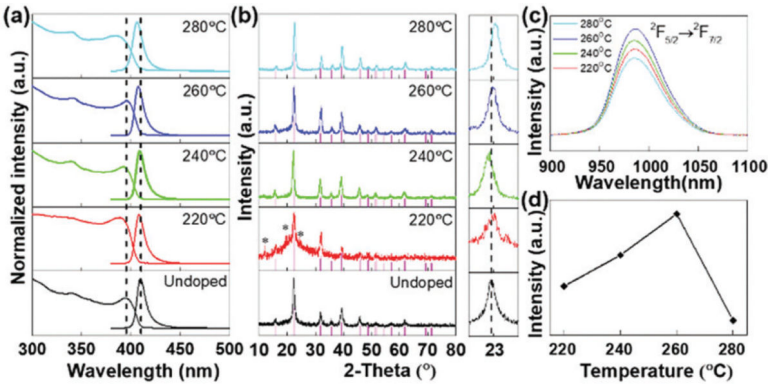

Fig. 1.

Optical properties and XRD characterization of the $CsPbCl_3:Yb^{3+}$ NCs synthesized at different reaction temperatures. (a) Absorption and intrinsic emission spectra. (b) XRD patterns and amplified views around 23°. (c) NIR emission spectra and (d) integral emission intensities of the $CsPbCl_3:Yb^{3+}$ NCs at different reaction temperatures.

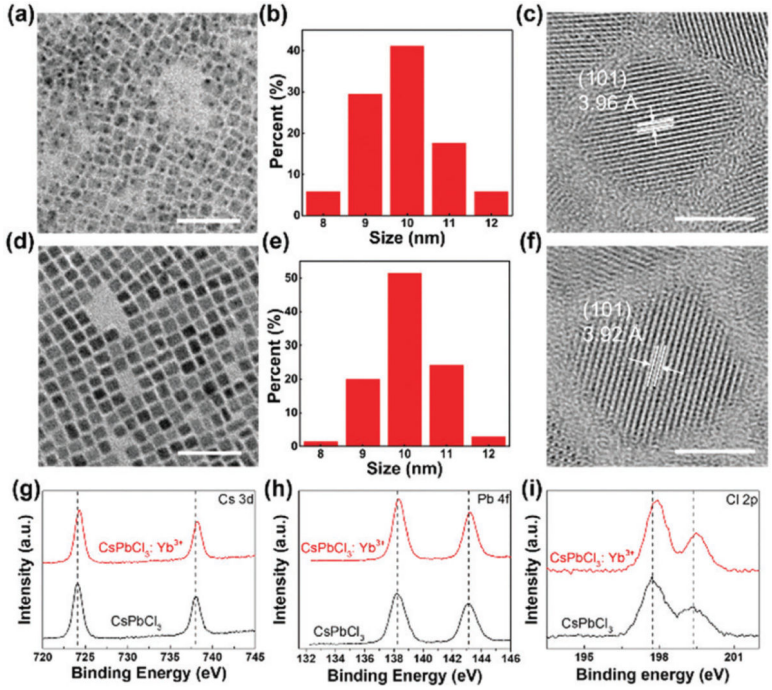

Fig. 2.

TEM (scale bar 50 nm) images, size distribution and HRTRM images (scale bar 5 nm) of the undoped $CsPbCl_3$ NCs (a–c) and $CsPbCl_3$:Yb^{3+} NCs (d–f), respectively. High resolution XPS spectra of the $CsPbCl_3$ (black) and $CsPbCl_3$:Yb^{3+} (red) NCs for (g) Cs 3d, (h) Pb 4f, (i) Cl 2p.

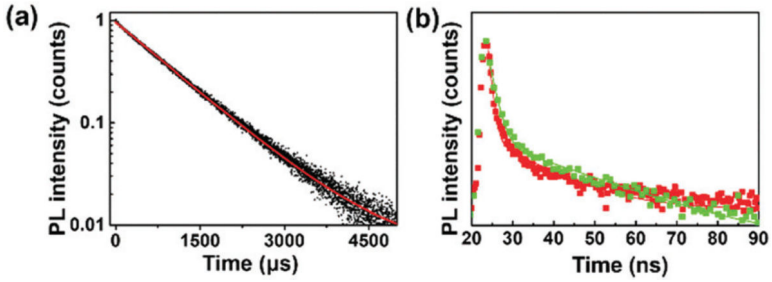

Fig. 3.

(a) Time-resolved PL decay profile of $^2F_{5/2} \rightarrow {}^2F_{7/2}$ of the Yb^{3+} ions in the $CsPbCl_3:Yb^{3+}$ NCs. (b) Time-resolved band edge emission decay profiles of the $CsPbCl_3$ (red) and $CsPbCl_3:Yb^{3+}$ (green) NCs.

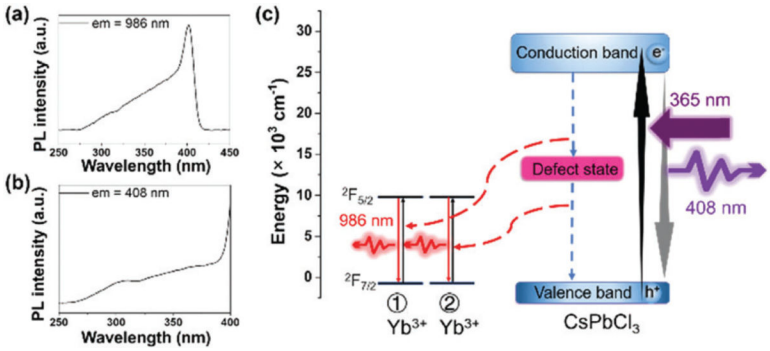

Fig. 4.

(a) Excitation spectrum of the $CsPbCl_3:Yb^{3+}$ NCs monitored at 986 nm. (b) Excitation spectrum of the $CsPbCl_3:Yb^{3+}$ NCs monitored at 408 nm. (c) Proposed energy transfer mechanism for the $CsPbCl_3:Yb^{3+}$ NCs.

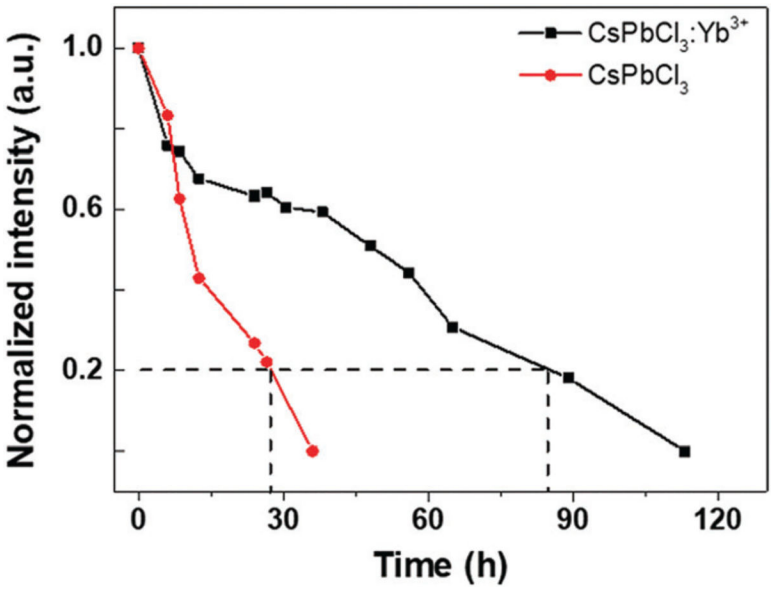

Fig. 5.
PL decrease of the $CsPbCl_3$ and $CsPbCl_3$:Yb^{3+} NCs under 365 nm UV light irradiation.